COO-3077-30
MF-71

Courant Institute of
Mathematical Sciences

Magneto-Fluid Dynamics Division

A New Approach to Magnetohydrodynamic Stability
II. σ-Stable Diffuse Pinch Configurations

P. H. Sakanaka and J. P. Goedbloed

AEC Research and Development Report

Plasma Physics
July 1973

New York University

UNCLASSIFIED

New York University
Courant Institute of Mathematical Sciences
Magneto-Fluid Dynamics Division

MF-71 COO-3077-30

A NEW APPROACH TO MAGNETOHYDRODYNAMIC STABILITY

II. σ-STABLE DIFFUSE PINCH CONFIGURATIONS

P. H. Sakanaka and J. P. Goedbloed*

July 1973

---

* On leave of absence from FOM-Instituut voor Plasma-Fysica, Jutphaas, The Netherlands.

This work was supported by the U.S. Atomic Energy Commission inder Contract No. AT(11-1)-3077. It was partly supported by Euratom, FOM, and ZWO.

UNCLASSIFIED

ABSTRACT

On the basis of the theory of σ-stability, developed in a previous paper, a classification of high-shear σ-stable diffuse pinch configurations is obtained by numerical solution of the Euler equation corresponding to the modified energy principle. Toroidal effects are introduced by putting a lower bound on the magnitude of the poloidal field in order to assure toroidal equilibrium and by deriving and employing the proper generalization of the Kruskal-Shafranov limit for $m = 1$ unstable configurations. The classification of high-shear σ-stable configurations consists of five different types, viz. Tokamak, B_θ-reversed pinch, screw pinch, combined pinch, B_z-reversed pinch. Among the significant new results are: complete stability of some of the Tokamak configurations for β up to 4%, a stable high-β (30%) B_θ-reversed pinch configuration that has not been investigated before, a stable diffuse screw pinch with $\beta = 30\%$ when currents are allowed to flow at the wall and with $\beta = 8\%$ with vanishing current at the wall, the possibility of containing diffuse high-β $m = 1$ stable plasmas without B_z-field reversal or pressure minimum on axis. Here, σ-stability refers to times needed for fusion.

1. Introduction.

In a preceding paper[1)] [henceforth quoted as I] we introduced the concept of σ-stability, observing that for thermonuclear confinement of plasma it is not necessary to demand absolute stability but that it is sufficient that perturbations do not grow faster than $e^{\sigma t}$ when $1/\sigma$ corresponds to some characteristic time needed for fusion. In this paper the stability of the diffuse linear pinch is reinvestigated on the basis of this enlarged stability concept, where the aim is to derive a, as complete as possible, classification of σ-stable equilibria. The significance of this approach rests upon the fact that in ideal magnetohydrodynamics many unstable modes occur which have vanishingly small growth rates, so that the class of σ-stable equilibria which are acceptable in fusion devices is much wider than the class of absolutely stable equilibria. In demanding absolute stability one, therefore,dismisses a number of interesting experimental possibilities which could have advantages other than following from ideal MHD.

In the usual stability analysis of the diffuse linear pinch a local criterion (Suydam's[2)] criterion) is fairly easily obtained, but it is well-known that local stability does not guarantee global stability. In order to establish global stability one has to solve a differential equation, where all the details of the equilibrium distribution of magnetic field components and pressure enter. Stability then often turns out to be such an extremely sensitive function of the equilibrium profiles that the relevance for experimental situations becomes very doubtful. For this reason, a σ-stability analysis is much more satisfactory, because many of the subtleties of ideal MHD connected with the singular behavior of the equations at marginal stability disappear. Consequently, it becomes possible to construct bands of σ-stable equilibrium profiles, so that a certain amount of imprecision is allowed for a profile in order to be σ-stable. Such an approach seems to be a proper theoretical reflection of the fact that experimentally profiles cannot be produced with any desired amount of precision.

The present paper is entirely devoted to a numerical investigation of σ-stable diffuse linear pinch configurations. The analysis is based on the oscillation theorem for σ-stability derived in I, Sec. 3a. This theorem is analogous to Newcomb's$^{3)}$ theorems pertaining to marginal stability, but it has the important advantage that no singularities are encountered so that a faster numerical calculation is possible. Thus, computer time is saved for the purpose of scanning many equilibrium profiles. The only restriction on the form of the chosen equilibrium profiles has been that it should satisfy Suydam's criterion. The implication of this restriction has been discussed at length in I, Sec. 4. For the present paper, it implies that we are restricting the analysis to intermediate- and high-shear configurations where violation of Suydam's criterion in most cases leads to rapidly growing nonlocalized

$m = 1$ modes having large growth rates. Therefore, Suydam's criterion provides a convenient way of preselecting equilibrium profiles for the intermediate- and high-shear cases.

It should be clear from the preceding discussion that σ-stable diffuse pinch configurations are to be found in two broad categories, viz. high-shear configurations and low-shear configurations. The first class is treated in this paper, where the returning feature will be improved stability by increasing the shear. The existence of the second class of low-shear σ-stable configurations has been indicated by Grad.4) It will be the subject of future numerical investigations. The reason for a separate treatment is that the rules for obtaining and optimizing the two types of configurations are completely different. For the high-shear configurations Suydam's criterion acts as a necessary condition for σ-stability (except in a few cases to be found in the text). Toroidal periodicity is taken into account only for $m=1$, the unstable regions for higher m normally being broad and sometimes overlapping. For the low-shear configurations, on the other hand, Suydam's criterion is not relevant and the higher m modes are stabilized by toroidal periodicity. In this case, σ-stability provides the connection between favorable closed-line stability results and the possibility of low-shear σ-stable systems.

Most of the older investigations on the linear pinch have been restricted to sharp-boundary and constant-pitch models.5) With the exception of Ref. 6, these studies have only more recently been extended to include numerical calculation of growth rates of instabilities for completely diffuse models[7),8),9)]. One of the merits of the numerical approach is that one can easily check whether the results obtained from special models have a more general validity. Although a number of results do stand this test, there is also a fair amount of deep-rooted misconceptions based on the results obtained from special models, e.g.: that the stability of the $m = 1$ mode does not very much depend on the details of the current distribution, that violation of Suydam's criterion leads only to localized modes, that the θ-pinch is a singularly isolated stable equilibrium, that sharp-boundary pinches are more stable than diffuse ones, or vice versa, that one can distinguish between kinks and interchanges, that the worst perturbations are incompressible, that incompressibility is a good approximation if the longitudinal field is large, that the generalization of the Kruskal-Shafranov limit for a diffuse pinch can be expressed in terms of a local criterion for q, etc., etc. It is an easy matter to produce for each of these statements a profile which contradicts it.

The main problem in abstracting general information on the question about what is good and what is bad for stability is the fact that stabilizing and destabilizing factors cannot be separated. E.g., a current parallel to the magnetic field drives instabilities but also creates stabilizing shear, so that the stability just depends on the details of the current distribution. Our approach to this problem here is to generate as many different σ-stable profiles as possible, in this way abstracting information on this question.

This paper is arranged as follows. In the next section the basic equations are given and the numerical procedure is outlined. In Sec. 3 simple conditions for toroidal equilibrium and stability are introduced as additional constraints in the theory. In Sec. 4, which constitutes the core of this paper, the obtained σ-stable equilibrium profiles are shown. These equilibria include Tokamak, B_θ-reversed pinch, screw-pinch, combined pinch, B_z-reversed pinch, and different hybrid forms of these configurations. Roughly two categories are obtained depending on whether or not toroidal periodicity has to be taken into account. In order to obtain a complete survey, we have not hesitated to include known results as well. In Sec. 5 some very unstable but realistic configurations are also shown, serving as a warning against premature optimism.

2. Procedure.

We investigate numerically the σ-stability of diffuse linear pinch configurations. The equilibria are described by the three profiles $p(r)$, $B_\theta(r)$, and $B_z(r)$, which are connected through the equilibrium equation

$$(p + \frac{1}{2} B^2)' + B_\theta^2/r = 0. \tag{1}$$

Fixing the value of β, where

$$\beta = \frac{p(0)}{p(0) + B^2(0)/2}, \tag{2}$$

this leaves two of the three profiles to be chosen arbitrarily, e.g., p and $\mu = B_\theta/rB_z$. In order to reduce the number of possibilities further we restrict the analysis to those equilibria for which the pressure is a monotonically decreasing function of r ($p'<0$) and which are Suydam-stable. The first restriction is a natural one in view of the fact that we are interested in confined plasmas, whereas the second restriction was discussed at length in I, Sec. 4. From Suydam's criterion

$$p' + \frac{1}{8} r B_z^2 (\frac{\mu'}{\mu})^2 > 0 \tag{3}$$

we now have that $|\mu'/\mu^2| \neq 0$ everywhere if $p' < 0$, so that μ also has to be a monotonic function of r.

This leads to the basic possibilities depicted in Fig. 1. The function μ can be a positive decreasing function of r (Fig. 1A), it can change sign when B_θ passes through zero (Fig. 1B), it can be a positive increasing function (Fig. 1C,D), or it can go to infinity and change sign when B_z passes through zero (Fig. 1E). The cases C and D will be distinguished later on the basis of toroidal considerations. For convenience, we have attached familiar names to these configurations which does not necessarily imply that the experimental confinement systems known by these names do have precisely the depicted profile. We shall show that in each of the indicated group of profiles of Fig. 1 σ-stable configurations exist with acceptable values of σ and β as regards to fusion. Many of the σ-stable configurations turn out to be smoothly transformable into one another, so that a lot of hybrid forms can be obtained. Only the most basic types will be presented here.

Different equilibrium profiles are generated and tested with respect to σ-stability. The numerical procedure is based on the theorem for σ-stability derived in I, Sec. 3a. For a certain range of values of m and k one has to integrate the σ-Euler equation

$$\begin{aligned}
&\frac{d}{dr}\left[\frac{(\rho\sigma^2+F^2)\left\{\rho\sigma^2(\gamma p+B^2)+\gamma pF^2\right\}}{D}\frac{1}{r}\frac{d}{dr}(r\xi_r)\right] \\
&-\left[\rho\sigma^2+F^2+r\left(\frac{B_\theta^2}{r^2}\right)'-4\frac{k^2B_\theta^2}{r^2}\frac{\rho\sigma^2B^2+\gamma pF^2}{D}\right. \\
&\qquad\left.+r\left\{2\frac{kB_\theta}{r^2}\left(\frac{mB_z}{r}-kB_\theta\right)\frac{\rho\sigma^2(\gamma p+B^2)+\gamma pF^2}{D}\right\}'\right]\xi_r=0
\end{aligned} \tag{4}$$

where $$F = mB_\theta/r + kB_z, \tag{5}$$

$$D = \rho^2\sigma^4 + \rho\sigma^2(m^2/r^2+k^2)(\gamma p+B^2) + (m^2/r^2+k^2)\gamma pF^2, \tag{6}$$

subject to the boundary condition

$$r\xi_r = 0 \quad \text{at} \quad r = 0. \tag{7}$$

If the obtained solution has no zero in (0,a) the pinch is σ-stable for that value of m and k, if there is a zero the pinch is σ-unstable, whereas a zero at $r = a$ implies that there exists an eigenvalue $\omega^2 = -\sigma^2$. It is clear that the numerical procedure can easily be extended to calculate growth rates if that is desirable. The range of values of m and k to be tested for σ-stability can be reduced considerably by realizing that only the lower-m modes can be unstable if Suydam's criterion is satisfied (I,Sec.4), whereas the width of the unstable k-region usually is only of the order $|\mu m|$. This facilitates a rapid test for σ-stability.

The values of σ to be chosen depend on the purpose of the σ-stability analysis. For a specific experiment, a relevant choice would be $\sigma = {}^1/\tau_{decay}$, where τ_{decay} is the available time as determined by the decay of the external or plasma currents. From a σ-stability analysis one could then find out whether the decay of plasma currents could be due to MHD instabilities or should be sought elsewhere. Here, we choose σ to correspond to times needed for fusion according to Lawson's criterion, so that we obtain a classification of diffuse linear pinch configurations which are stable on that time-scale. The parameter

σ enters the analysis only through the dimensionless quantity

$$\Sigma^2 = \frac{4\pi\rho\sigma^2 a^2}{B_o^2} , \tag{8}$$

which has to be fixed by a reasonable choice of the values of ρ, a, and B_o. For a hydrogen plasma the connection between the e-folding time τ and the value of Σ is given by the relation

$$\tau = 4.6 \times 10^{-12} \frac{an^{1/2}}{B_o} \Sigma^{-1} \text{ [sec]}, \tag{9}$$

where a is given in cm, n in particles per cm^3, B_o in Gauss. An example is given in Table I for a plasma with a density somewhere in between usual Tokamak and pinch densities. In order to distinguish between σ-stability, where growth at most like $e^{\sigma t}$ is allowed, and actual growth rates of instabilities, we indicate eigenvalues $\omega^2 < 0$ of unstable normal modes $e^{i\omega t}$ by the dimensionless quantity $-\Omega^2 = \Sigma^2$ as given by Eq. (8).

σ-stable plasmas of thermonuclear interest are obtained for values of Σ^2 ranging from 10^{-10} to 10^{-12}. It should be noticed that the precise value of Σ^2 does not enter the analysis in a very critical manner. The important feature is just that the mentioned range of values of Σ^2 is far away from the range 10^{-2} to 10^{-4}, where violent kink-instabilities destroy the plasma immediately whereas it is also far away from $\Sigma^2 = 0$, where the singular nature of the marginal stability analysis causes the stability question to be a very critical one, depending sensitively on the equilibrium profiles. In the σ-stability analysis, on the other hand, stable profiles occur in bands, so that important experimental questions can be answered, such as "How accurate should a given profile be produced in order to be stable during a given time interval?". In Section 5 it will be shown that this band is very narrow. However there are an infinite number of parallel σ-stable bands, hereafter called σ-stable striae of equilibrium profiles, covering continuously the space between two σ-stable profiles of a same class. There are also a number of σ-stable striae which cross other σ-stable striae, thus forming a mesh of σ-stable striae. An example of such σ-stable striae of equilibrium profiles is given in Fig. 2, where the pressure profile is kept fixed and the B_z-profile is changed continuously from a stable one without a field-reversal to a stable one with a field-reversal. In between these two cases a whole variety of σ-stable fields occur.

From Eq. (4) it is evident that the density profile $\rho(r)$ also enters the σ-stability analysis because σ only appears through the combination $\rho\sigma^2$ in the equation. We are entirely free to choose this profile, or the temperature profile, because there is no equilibrium equation fixing it. However, the results are very insensitive to the choice of this function (at least, as long as it does not become very small), so that there is little point in considering $\rho(r)$ as an additional profile in the classification. For convenience, we have chosen a constant density throughout the whole region (0,a), which corresponds to a temperature profile having the same radial dependence as the pressure profile. The advantage of this choice is that one can easily renormalize the value of $\sum^2$ if one wishes to take the influence of lower density regions into account. Moreover, we thus have chosen to represent the outer regions of a pinch as a pressureless plasma rather than a vacuum,in this way avoiding difficulties associated with the limit $\rho \to 0$. The latter difficulties stem from the fact that in this limit $W^{\sigma} \to W$, so that the singular marginal stability analysis is recovered. For a real vacuum one can avoid singularities by transforming to the variable Q_r (the radial component of the magnetic field perturbation), but in reality the outer region of a pinch is seldom properly approximated as a vacuum and for some configurations this region even carries large equilibrium currents. In this case, the transformation to the variable Q_r still makes sense if the marginal stability with respect to tearing modes is considered, but an investigation of σ-stability with respect to these resistive instabilities would require the study of the full resistive MHD equations which goes well beyond the scope of present analysis.

3. Toroidal effects.

A naive scheme for the maximization of β with respect to the stability of a diffuse linear pinch automatically leads to the θ-pinch ($B_z = 0$). This result is trivial because the θ-pinch is stable for arbitrary pressure-profiles including those for which $\beta = 1$. As far as ideal MHD stability is concerned, this would then be the very comforting end of the investigation, but it is well-known that life is not that simple and the unavoidable end-losses present in a linear θ-pinch confirm this conventional wisdom. In order to eliminate these losses one bends the θ-pinch into a torus, discovers that there is no toroidal equilibrium with a longitudinal field alone, hence, introduces a poloidal field component, and finally discovers that a vast area of new possibilities has been opened up, but that the nice stability properties of the linear θ-pinch have been lost completely. The reason is that the poloidal field necessary for toroidal equilibrium is so large that it introduces rapidly growing $m = 1$ instabilities for most of the configurations.

It is clear that a stability analysis of a diffuse linear pinch which is undertaken with an eye on the application to toroidal devices has to take into account the most obvious toroidal effects of equilibrium and stability. These effects are twofold. Firstly, the condition for toroidal equilibrium puts a lower bound on the magnitude of B_θ. Secondly, the finite length of the machine introduces a discretization of the possible wavenumbers k in longitudinal direction, because the wavelength has to fit into the torus. The first of these is unfavourable for stability, because it involves a departure from the stable θ-pinch profiles, whereas the latter is favourable because it eliminates a number of possible unstable modes. The question of stability thus becomes a delicate optimization problem where the profiles are the variables and toroidal equilibrium conditions act as constraints.

On the basis of these considerations the classification of diffuse linear pinch profiles given in Fig. 1 can be subdivided into two classes, viz. those for which $B_\theta << B_z$ where toroidal effects are important (A,B,C), and those for which $B_\theta \sim B_z$ where toroidal effects may be neglected (D,E). Strictly speaking, the stability theory of the diffuse linear pinch is only a good approximation for the latter class of profiles, whereas the first class requires a consistent toroidal study of both equilibrium and stability. Such a study is not undertaken here and has not been undertaken yet, to our knowledge. Instead, we just introduce the mentioned most obvious effects of toroidal equilibrium and stability as extraneous constraints in the stability theory of the diffuse linear pinch. There is no doubt that the results obtained this way will undergo substantial modification in the correct consistent treatment, but we believe that an understanding of the complex influence of the profiles on the stability, already present in the simple straight geometry, is imperative to progress for more complicated geometries.

The limitation on B_θ posed by the toroidal equilibrium requirements is taken from the literature by the method of averaging the results of different authors. There seems to be agreement$^{10),11),12)}$ on the fact that fundamental limitations on β as far as toroidal equilibrium is concerned do not exist, but that a number of practical considerations pose a limit which is conveniently written as

$$\beta_\theta < A, \tag{10}$$

where A is the aspect ratio of the torus, $A = R/a$, and

$$\beta_\theta = \frac{2p(0)}{B^2_{\theta\ \max}} . \tag{11}$$

This result seems plausible enough in as far as it expresses that the field B_θ, which is compressed against the wall, should be large enough to counterbalance the expansion force of the plasma. It is clear, however, that it is no more than an order of magnitude estimate of an effect which is just as profile-dependent as the stability results we are reporting. We simply take this limit as given, but notice that the stability results improve to the extent that one is able to keep the plasma in equilibrium with a smaller poloidal field than that given by Eq. (10).

The main stabilizing effect of the toroidal geometry is the possibility to eliminate $m = 1$ modes with wavelengths larger than the circumference of the torus. This effect is known under the name Kruskal-Shafranov limit and requires a short exposition.

The original derivation[13)] concerned a sharp-boundary pinch model of a homogeneous plasma separated from a vacuum region by surface currents creating a μ-profile as shown in Fig. 3. For $\beta << 1$ the $m = 1$ modes have a growth rate given by

$$\omega^2 \approx 2k[k+\mu(r_o)]v_A^2, \tag{12}$$

so that instability occurs for $|k| < |\mu(r_o)|$. This mode is eliminated if the first value of k compatible with toroidal periodicity falls outside the unstable region, i.e. if $k = 1/R > |\mu(r_o)|$ or $|\mu(r_o)R| < 1$. In terms of the variable $q = (\mu R)^{-1}$:

$$q(r_o) > 1. \tag{13}$$

The simplicity of this result suggests a general validity, which can be rejected, however, by means of the same model. For $\beta = 1$ the growth rate is given by

$$\omega^2 \approx k[k+2\mu(r_o)]\frac{2p}{\rho}, \tag{14}$$

so that instability occurs for $|k| < 2|\mu(r_o)|$ and the criterion for the absence of $m = 1$ instabilities becomes

$$q(r_o) > 2. \tag{15}$$

Hence, the idea behind the derivation is general, but the explicit form of the criterion itself is not.

The sharp-boundary model with a vacuum outside the plasma has some additional peculiarities illustrating that results obtained from special models can hamper an understanding of the general features. Take, e.g., a low β sharp boundary plasma surrounded by an ideally conducting wall. One shows that for reasonable wall distances the plasma is stable with respect to all modes except $m = 1$. Observing the Kruskal-Shafranov limit (13) would then lead to a completely stable configuration and one can even show that fairly high values of β are permitted. However, if one now tries to depart somewhat from the sharp boundary model, Fig. 3 clearly shows that one ends up with a μ-profile having a maximum at a position where the pressure gradient is large. Suydam's criterion is violated for such a configuration and the plasma becomes unstable with respect to rapidly growing $m = 2,3,\ldots$. instabilities. For this reason, our classification of σ-stable profiles of Sec. 4 will not list any configuration close to this model.

We now move to another class of special models, viz. Tokamak configurations (Fig. 1,A), and encounter another version of the Kruskal-Shafranov limit:

$$|q|_{min} > 1 \quad \text{or} \quad |\mu|_{max} R < 1. \tag{16}$$

This criterion is equally not general. That it is not necessary for stability of $m = 1$ modes is proved by the existence of completely stable B_z-reversed pinch configurations (Fig. 1,D), which have infinite values of $|\mu|_{max}$. That it is not sufficient is shown by the fact that a constant-pitch region around the axis is subject to $m = 1$ instabilities having k-values in a region around $k = -\mu(o)$, so that unstable modes with $|k| > |\mu|_{max}$ are not eliminated by the condition (16). The first example involves an increasing μ-profile, whereas the second one violates Suydam's criterion on axis.

Maybe then, the criterion is a general statement about configurations having a monotonically decreasing μ-profile and satisfying Suydam's criterion. There is a counter-example for this statement also, which is shown in Fig. 4. Depicted is the μ-profile for a B_θ-reversed pinch where μ is a decreasing function of r, passes through zero, and then takes on very large negative values. The σ-unstable region of k-values, corresponding to radial positions where $k = -\mu(r)$, is also indicated and is only slightly smaller than the 0-unstable region of k-values which extends up to $k = -\mu(o)$ on one side, but certainly not up to $k = -\mu(a) = |\mu|_{max}$ on the other side. Therefore, one may have $|\mu|_{max} R >> 1$ for this configuration and still stabilize the unstable $m = 1$ modes by toroidal periodicity. It might thus be that criterion (16) is the proper generalization of the Kruskal-Shafranov limit for configurations with a monotonically decreasing μ-profile, not crossing the axis, and satisfying Suydam's criterion (i.e., solely for Tokamak-like profiles indicated in Fig. 1, A). It is certainly a necessary criterion for this restricted class of configurations, because all $m = 1$ modes with $|k| < |\mu(0)|$ are unstable, as has been proved by Shafranov14) and Robinson15). However, we have not been able to exclude the possibility that $m = 1$ instabilities also might occur for $|k| > |\mu(0)|$, which would spoil the sufficiency of criterion (16).

For our purpose the only useful form of the toroidal periodic condition is the following, completely general but implicit, condition for the absence of the $m = 1$ instabilities. One easily shows that the pinch is stable for fixed m as $k \to \infty$. Consequently, the interval of unstable k-values has to be limited:

$$k_o < k < k_1 \; . \tag{17}$$

Writing $\bar{k} = \mathrm{Max}\left\{|k_o|, |k_1|\right\}$, the proper generalization of the Kruskal-Shafranov limit then becomes

$$1/R > \bar{k}, \quad \text{or} \quad A < (\bar{k}a)^{-1} \; . \tag{18}$$

This result applies to all configurations and, most important, is also valid in a σ-stability analysis. The interval (k_o, k_1) may contain stable subintervals (and we have examples where this is so), but the possibility of exploiting those is not considered here. However, they give rise to so-called stability windows which play a significant role for the low-shear case. The fact that the criterion is implicit is no drawback for the numerical analysis, because one has to check for the stability of $m = 1$, all k anyway. Of course, the width of the unstable region (k_o, k_1) is only of the order $|\mu|$.

In conclusion, the consideration of simple toroidal equilibrium and stability requirements expressed by the inequalities (10) and (18) leads to two entirely different classes of σ-stable configurations. Either $m=1$ is unstable and one has to optimize the configurations such that β is as large as possible, but that still the condition

$$\beta_\theta < A < (\bar{k}a)^{-1} \tag{19}$$

is satisfied. Or $m = 1$ is stable and toroidal effects do not present a serious restriction on the possible configurations. These two possibilities correspond to the cases (A,B,C) and (D,E) indicated in Fig. 1.

4. Classification of σ-stable configurations.

The discussion of the preceding section leads to the following classification:

- m = 1 unstable configurations, stabilized by toroidal periodicity, $B_\theta << B_z$:

A. Tokamak (Figs. 1A,5-8), decreasing μ,

B. B_θ-reversed pinch (Figs. 1B,9,10), decreasing μ with reversal,

C. Screw-pinch (Figs. 1C,11-12), increasing μ flattening in outer region;

- m = 1 stable configurations, stabilized by high shear, $B_\theta \sim B_z$:

D. Combined pinch (Figs. 1D,13), increasing μ,

E. B_z-reversed pinch (Figs. 1E,14), increasing μ with reversal.

Each of these configurations will be discussed on the basis of the numerical results.

The Figs. 5-14 show a selection of σ-stable configurations, where we have strived to maximize β, observing the restrictions posed by toroidal equilibrium. For each configuration we have shown: a) the basic characterizing profile $\mu(r)$, normalized for a wall radius a = 1, b) the functions $p(r)$, $B_\theta(r)$, and $B_z(r)$, which determine the equilibrium completely, c) the derived current profiles $j_\theta(r)$ and $j_z(r)$ which are of practical interest. We indicate the values of β and β_θ as defined by the Eqs. (2) and (11), and the value of $\sum^2$ as defined by Eq. (8). For the configurations that are m = 1 unstable we also give the maximum growth rate - Ω^2_{max} of the m = 1 instabilities and the maximum aspect ratio A_{max} for which criterion (18) is still satisfied.

A. Tokamak.

The sequence is started with two configurations (Figs.5,6) which exceed the limit (10) posed by toroidal equilibrium by some orders of magnitude. They have high values of β and the poloidal current is larger than the toroidal current. The purpose of these pictures is to show the smooth transition from θ-pinch to σ-stable Tokamak profiles. If one could keep these configurations in equilibrium by means other than increasing the poloidal field, one would have a high-β stable Tokamak with the additional advantage of enhanced heating by the poloidal current. These advantages, combined with the finding of Callen and Dory12) "that from magnetohydrodynamic equilibrium considerations alone there is no apparent limit on β_θ up to about A^2 and thus limit on β up to about unity", warrant a further study of the practical limitations on toroidal Tokamak equilibrium listed in the mentioned reference.

The next two pictures (Figs.7,8) show more standard Tokamak profiles. These represent σ-stable configurations with the highest values of β we could obtain without violating condition (10) for toroidal equilibrium. The profiles are the result of a subtle optimization process, where the condition (10) for toroidal equilibrium favors a large value of μ at the wall, the toroidal periodicity condition (18) for the absence of $m = 1$ modes favors a small value of μ on axis, but the stability conditions for a diffuse linear pinch in general demand a large shear, i.e., the difference $\mu(o) - \mu(a)$ as large as possible. For a Tokamak, where the μ-profile is decreasing without crossing the axis, these conflicting conditions lead to severe limitations of the possible values of β and one ends up with values of β of the order 0.03 to 0.04. The demonstration that Tokamak profiles exist which are stable with respect to $m = 2,3,...$ is due to Shafranov14).

In order to satisfy Suydam's condition at $r = 0$ the pressure profile has to be rather flat on axis, such as is given by $p \sim \exp(-Br^4)$. A consequence of this condition and the equilibrium equation (1) is the structure of the current profile j_θ, which tends to develop a reversal of the sign. More smooth j_θ profiles can be obtained by starting from a pressure profile like $p \sim \exp(-Ar^2-Br^4)$, but the result is evidently Suydam-unstable plasma on axis (See Sec.5, Fig.15).

B. B_θ-reversed pinch.

In view of the mentioned limitations on the permissible β in a Tokamak, originating as a result of conflicting conditions on the μ-profile, a logical step seems to consider monotonically decreasing μ-profiles which reverse sign. The first configuration (Fig.9) shows that this can be done by inducing currents of opposite direction through the outer regions of the pinch. The result is a μ-profile with very favourable properties for magnetohydrodynamic stability, viz. rather small values of μ on the average and still high shear. Accordingly, one can obtain stable configurations with $\beta = 0.3$, which is an order of magnitude larger than the possible values for a Tokamak. The $m = 1$ modes are still unstable, because μ is a decreasing function (see Sec.3), but they are eliminated by means of the toroidal periodicity condition, whereas the higher-m modes are stabilized by the presence of high shear. Toroidal equilibrium is due to the large poloidal field at the wall. The configuration can be considered as a superposition of Tokamak and screw pinch.

From a practical point of view the presence of large currents close to the wall seems unwanted. One can cure this by continuing the current profiles such that they decay to zero. In case the B_z-field is partly created by external currents, this will lead to a minimum in the μ-profile because the absolute value of μ for a vacuum field has to decay like $^1/r^2$. The associated instabilities have small growth rates so that σ-stability is still possible, but the value of β has to be reduced (see the similar effect for the screw pinch in Fig. 12). Another possibility is shown in Fig. 10. Here, there is no minimum in μ because the B_z-field is created exclusively by means of plasma currents, so that $B_z \to 0$ and $\mu \to \infty$ at the wall. The resulting high shear is favourable both for stability and toroidal equilibrium, so that the large values of β can be maintained. The configuration is $m = 1$ unstable, but we have already shown in the preceding section that the unstable region occurs for k-values which can be eliminated by means of the toroidal periodicity condition despite of the large value of μ at the wall.

The configuration of Fig. 10 can be looked upon as a superposition of Tokamak and combined pinch. The sequence of σ-stable profiles could be continued further with superpositions of Tokamak and B_z-reversed pinch, having then a μ-profile going through zero and infinity, but the increasing complexity of the current distributions (and, therefore, the associated necessity of complex circuit programming) makes such configurations of little practical use. From the completely different distributions of Figs. 9 and 10, it is clear that many more stable configurations with high values of β can be constructed. To our knowledge, stable B_θ-reversed pinches have not been considered before, neither theoretically nor experimentally.

C. Screw-pinch.

Another sequence of σ-stable profiles is obtained for increasing μ-profiles. Such configurations arise as a result of current distributions which are completely different from those of a Tokamak. In a Tokamak, the toroidal current has to be fairly peaked on axis in order to create a μ-profile with enough shear for stability$^{14)}$. In screw pinches, combined pinches, and B_z-reversed pinches the necessary shear is created in exactly the opposite manner, viz, by current densities that are small on axis and large in outward regions.

Such distributions arise as the result of imperfect induction of skin-currents (screw-pinch) or deliberate programming (B_z-reversed pinch).

The stability of screw-pinch configurations was considered first$^{16)}$ for a sharp-boundary model with a step-function for $\mu(r)$. Unlike the sharp-boundary model with a vacuum outside the plasma column (see Sec.3), this model can be turned into an acceptable diffuse configuration where the μ-profile is monotonically increasing. Such a profile is more or less the mirror-image of that of a Tokamak (cf. Figs.7 and 11), so that a similar optimization game can be played as before, but with slightly more favourable rules. The stability requirements on axis are now automatically satisfied because μ is small there. Toroidal equilibrium and linear pinch stability require a large value of μ at the wall, whereas the toroidal periodicity condition for the absence of $m = 1$ instabilities favors small values of $\mu(a)$. These conflicting conditions again restrict the possible values of β, but not to the same extent as for a Tokamak. Fig. 11 shows that stable configurations with values of β up to 0.3 can be obtained.

The unattractive feature of large current densities at the wall can be remedied as shown in Fig. 12. Because the fields have to transform into a vacuum configuration the function $\mu(r)$ now gets a maximum, so that Suydam's criterion is no longer satisfied. Since the pressure gradient is also small in that region the growth rates of the instabilities are still small, so that a σ-stable configuration is still possible. However, the value of β has to be reduced to about 0.08.

The necessity to observe the toroidal periodicity condition (18) for these configurations arises as a result of the fact that the shear, especially in the outer region of the pinch, is insufficient to stabilize the $m = 1$ mode. This is even more salient for the case that the μ-profile has a maximum like in Fig. 12. For this case, a proof has been given15) for the instability of the $m = 1$ mode, even if $p' = 0$ (so, it is a distinct phenomenon from violation of Suydam's criterion), similar to the proof for monotonically decreasing μ-profiles. The growth rates of these instabilities are quite large (cf. the values of $-\Omega^2$ in Figs. 11 and 12 with table I), so that it is imperative to satisfy condition (18). An alternative cure of these instabilities is to enhance the shear by increasing B_θ and decreasing B_z in the outer regions of the pinch. This leads to the next class of profiles.

D. Combined pinch.

A completely new class of configurations is obtained if one increases the shear and the ratio B_θ/B_z such that the $m = 1$ modes become stable. For these configurations toroidal equilibrium and stability considerations can be neglected and one has to deal with the stability of the diffuse linear pinch alone. A continuous transition from screw-pinch to combined pinch and B_z-reversed pinch has been described in Ref. 4 by means of a sharp boundary model with force-free currents outside the plasma column. If one insists upon having vanishing current densities at the wall, this transition is much less continuous and one finds that only one type of configuration survives which has a monotonically increasing μ-profile is stable for $m = 1$, and has no current at the wall. This is the combined pinch$^{17)}$ where the B_z-field tends to zero at the wall so that $\mu(a) \to \infty$. The resulting configuration shown in Fig. 13 is one of the nicest we encountered. It is a pure pinch configuration where confinement is solely due to the interaction of plasma currents and the wall. In the equilibrium state, no external current is present. The very large shear stabilizes all modes, including $m = 1$. The current distribution is naturally obtained by smoothing a sharp boundary stabilized z-pinch with a trapped B_z-field, surface currents and no B_z-field outside the plasma column (i.e., a step function $0 - \infty$ for $\mu(r)$). On the basis of the latter model, the possiblity of stable confinement of plasma with high values of β has been realized as early as 1957$^{18)}$.

E. B_z-reversed pinch.

The large shear of the combined pinch can even be exceeded if one allows for negative values of the B_z-field in the outer region of the pinch. The resulting B_z-reversed configurations 8), 15), 19), shown in Fig. 14, has the highest possible shear in the sequence of configurations with monotonically increasing μ-profiles, like the B_θ-reversed pinch in the sequence of monotonically decreasing μ-profiles. The possible values of β are, therefore, comparable for both field-reversed pinches, i.e. 0.2 - 0.3. Like in the combined pinch, the current profiles nicely decay to zero at the wall, so that the outermost region has a vacuum configuration. In the equilibrium state, the reversed B_z-field is maintained by an external poloidal current of opposite sign with respect to the plasma j_θ-current. As shown in Ref. 15, the wall position and the amount of field reversal determine the stability in such a way that the allowable percentage of the field reversal decreases if the wall position is increased, and vice versa. Therefore, the sequence of configurations with decreasing μ-profile naturally ends here, because the introduction of more shear apparently is not possible without at the same time introducing rapidly growing current-driven instabilities.

The given profiles in Fig. 14 differ in one important aspect from the ones studied in Ref. 15, which have a hollow pressure profile and a j_z-current profile which is peaked on axis. Here, the features are just reversed, viz. the pressure has a maximum on axis and the j_z-current has a maximum off-axis. Although both configurations have comparable stability properties, one of them could be a preferred equilibrium arising in the process of creation and diffusion of the plasma. 20)

5. Unstable configurations.

In order to arrive at a balanced conclusion, it seems appropriate also to expose the other side of the picture. For that purpose, we have chosen three representative unstable configurations which can well be distinguished from their stable counterparts, but are close enough to feel uncomfortable.

In Fig. 15 an unstable Tokamak configuration is shown together with a stable one. The unstable configuration deviates from the stable one in that the pressure decays faster on axis and the poloidal field is more concentrated towards the axis, but the deviation does not seem to be very large until one considers the more detailed information given in the derived quantities μ, j_θ, j_z and the Suydam function $S = 1 + \frac{8p'}{rB_z^2} (\frac{\mu}{\mu'})^2$ given in Fig. 16. It turns out that the instability is caused by violation of Suydam's criterion on axis, so that there is instability for all m (except $m = 1$ which is still absent because of toroidal periodicity). The growth rates are very large.

In Fig. 17 an unstable screw-pinch is shown together with a stable one. Again, the profiles are rather close, but the derived quantities (Fig. 18) give much more information. For a screw-pinch configuration violation of Suydam's criterion on axis would not matter very much because μ is small there, so that the growth rate is small and a large number of higher -m modes are eliminated by toroidal periodicity. However, instability is now induced by decreasing the current density close to the wall so that a region of small shear develops.

Hence, although Suydam's criterion is satisfied throughout the plasma, het higher-m modes are unstable having rather large growth rates.

Finally, we present in Fig. 19 an example which specifically has been constructed for the purpose of showing the intricacies of the problem. We show an $m = 1$ unstable combined pinch configuration which is extremely close to a σ-stable one but still has very large growth rates. From the equilibrium profiles in Fig. 19 it would even be impossible to predict which of the two is the stable and which is the unstable configuration. Figure 20 reveals how this example was constructed. The current profiles were provided with a small dent such that a tiny plateau in the μ-profile was produced. Consequently, in that small region Suydam's criterion is violated and the configuration becomes unstable with respect to a gross $m = 1$ mode having some tendency to localize in the Suydam-unstable region. This shows that σ-stable bands of equilibrium profiles only occur for profiles that are close with respect not only to p, B_θ, and B_z, but also with respect to j_θ and j_z.

Whether dissipative effects provide sufficient smoothing of the profiles in order to prevent the occurrence of situations like just described is an open question. On the other hand, the eigenfunctions also might be required to be sufficiently smooth. Numerically, artificial smoothing of the eigenfunctions can easily be obtained by putting an upper bound on the allowable values of the radial derivative of ξ_r, thus eliminating local instabilities. Such a procedure enlarges the class of σ-stable profiles significantly and, moreover, produces broad bands of σ-stable profiles. This heuristic procedure might find a justification in a more general description of the plasma, incorporating finite-Larmor radius effects.

The given examples suffice to show that categoric answers about which configurations are bad and which are good with respect to stability cannot be given.

6. Conclusion.

On the basis of the σ-stability theory of the diffuse linear pinch, supplemented with simple toroidal equilibrium and stability requirements, a classification of σ-stable high-shear configurations has been given, which we believe is fairly complete. Five different groups of configurations are obtained characterized by the function $\mu(r)$. In each of these groups a number of σ-stable configurations exist which have rather high values of β. However, highly unstable configurations with equilibrium profiles very similar to the stable ones also occur (Sec. 5) and it seems very difficult to avoid these unstable states. It is possible to refine the description of the plasma considerably, especially by taking toroidal curvature and resistive effects into account, but the mentioned problem will remain. Its solution will require a dynamical theory of the pinch abolishing the artificial separation of plasma equilibrium and stability.

Acknowledgments

The authors are indebted to Professors Harold Grad and Harold Weitzner for constructive criticism and for suggesting this investigation.

This work was supported by the U.S. Atomic Energy Commission under Contract No. AT(11-1)-3077. It was partly supported by Euratom, FOM, and ZWO.

References

1. Goedbloed, J.P. and Sakanaka, P.H.,

2. Suydam, B.R., Proceedings of the Second United Nations International Conference on the Peaceful Uses of Atomic Energy, Vol.31, Geneva (1958) 157.

3. Newcomb, W.A., Ann. Phys. (N.Y.) 10 (1960) 232.

4. Grad, H., to be published.

5. See references in Goedbloed, J.P., Physica 53 (1971) 412, 501, 535.

6. Hain, K. and Lüst, R., Z. Naturforsch. 13a (1958) 936.

7. Freidberg, J.P., Phys. Fluids 13 (1970) 1812.

8. Bodin, H.A.B., Butt, E.P., Crow, J.E., Irons, F.E., Junker, J., Newton, A.A., and Robinson, D.C., in Plasma Physics and Controlled Nuclear Fusion Research (International Atomic Energy Agency, Vienna, 1971) Vol. 1, p. 225.

9. Goedbloed, J.P. and Hagebeuk, H.J.L., Phys. of Fluids 15 (1972) 1090.

10. Mukhavatov, V.S. and Shafranov, V.D., Nuclear Fusion 11 (1971) 605.

11. Strauss, H.R., Phys. Rev. Let. 26 (1971) 616.

12. Callen, J.D. and Dory, R.A., Phys. Fluids 15 (1972) 1523.

13. Kruskal, M.D., Johnson, J.L., Gottlieb, M.B., and Goldman, L.M., Phys. Fluids 1 (1958) 421.

14. Shafranov, V.D., Zh. Tekh. Fiz. 40 (1970) 241 [Sov. Phys. Tech. Phys. 15 (1970) 175].

15. Robinson, D.C., Plasma Phys. 13 (1971) 439.

16. Schuurman, W., Bobeldijk, C., and DeVries, R.F., Plasma Physics 11 (1969) 495.

17. Whiteman, K.J., Plasma Physics 7 (1965) 293.

18. Tayler, R.J., Proc. Phys. Soc. (London) *B70* (1957) 1049.

19. Robinson, D.C. and King, R.E., in *Plasma Physics and Controlled Nuclear Fusion Research* (International Atomic Energy Agency, Vienna, 1968) Vol. *1*, p. 263.

20. Haberstich, A., private communication.

Table I

The relation between $\sum^2$, $-\Omega^2$ and e-folding times τ for $a = 100$ cm, $n = 10^{15}$ protons cm^{-3}, $B_o = 144$ kG.

$\sum^2, -\Omega^2$	$\tau = 10^{-7} \sum^{-1}$ sec	
10^{-12}	100 m sec	Thermonuclear plasma
10^{-10}	10 m sec	
10^{-8}	1 m sec	
10^{-6}	100 μ sec	
10^{-4}	10 μ sec	
10^{-2}	1 μ sec	kink-disrupted plasma

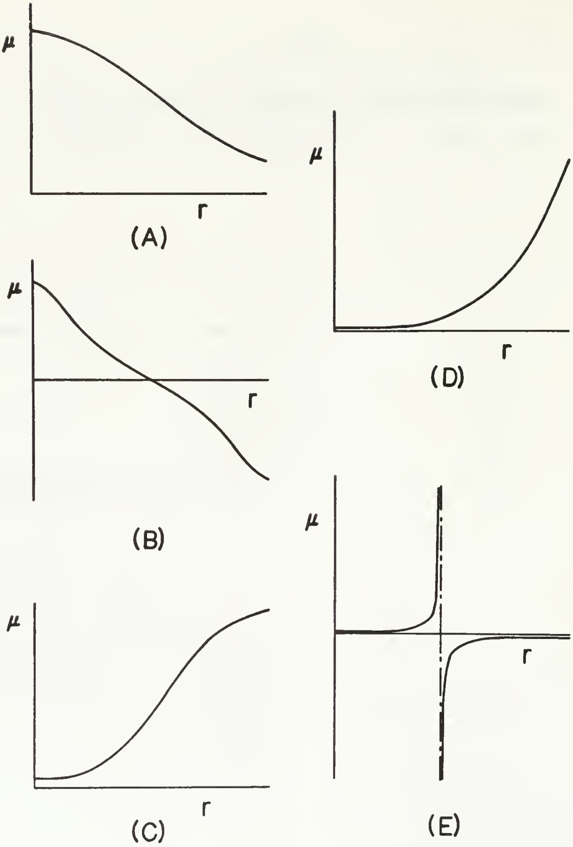

Fig. 1. Classification of linear pinch configurations according to μ-profile. A. Tokamak; B. B_θ-reversed pinch; C. Screw-pinch; D. Combined pinch; E. B_z-reversed pinch.

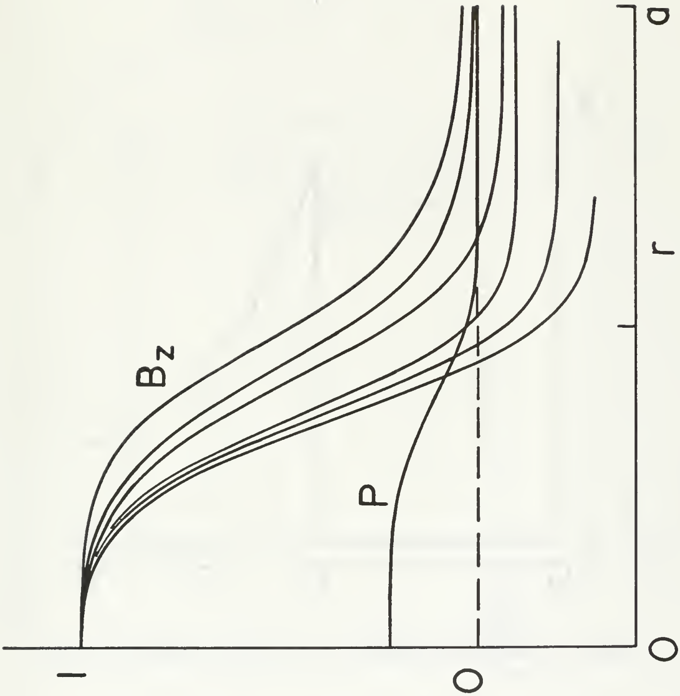

Fig. 2. Striae of σ-stable profiles, $\beta = 0.10$, $\beta_\theta = 0.23$ and $\sum^2 = 4 \times 10^{-12}$.

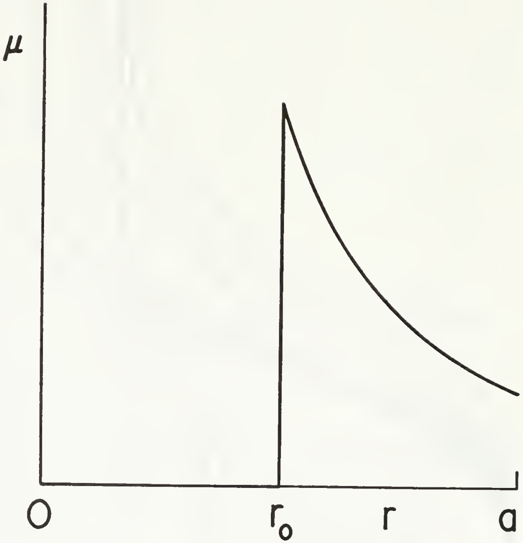

Fig. 3. Sharp-boundary model for a pinch surrounded by vacuum.

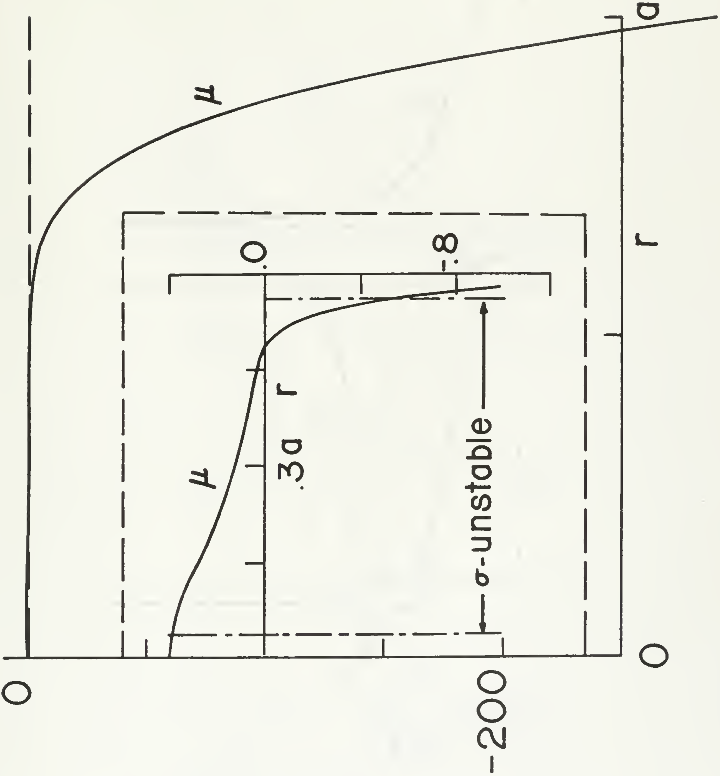

Fig. 4. μ-profile for a B_θ-reversed pinch. In box is the detail of μ-profile near origin.

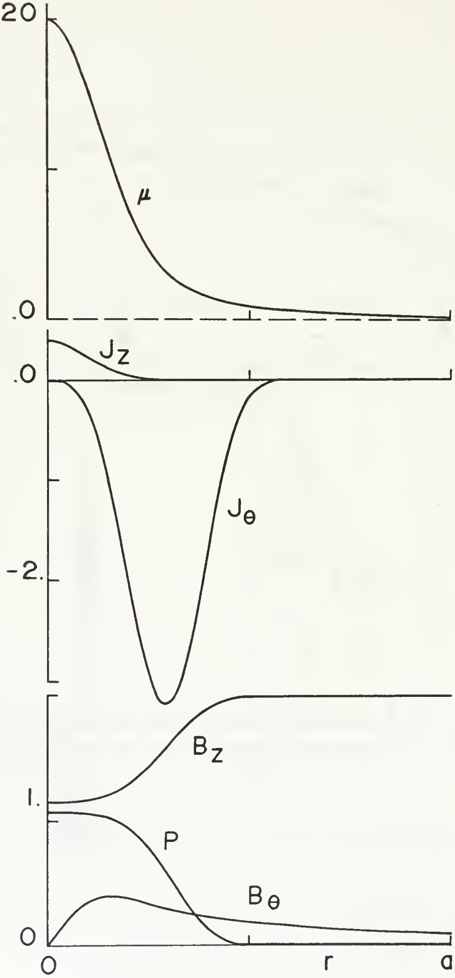

Fig. 5. Non-equilibrium Tokamak, $\beta = 0.67$, $\beta_\theta = 2 \times 10^4$, $A_{max} = 5.0$, $\sum^2 = 6.4 \times 10^{-11}$, $\Omega^2_{max} = - 1.9 \times 10^{-4}$, m = 1 unstable.

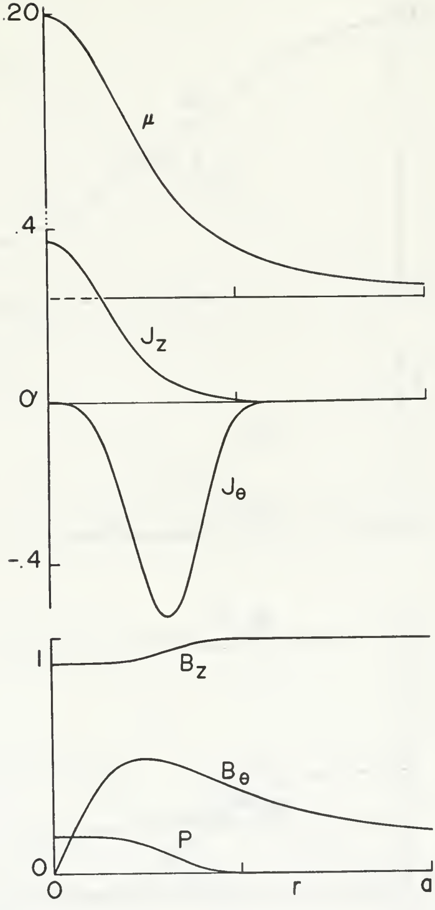

Fig. 6. Non-equilibrium Tokamak, $\beta = 0.20$, $\beta_\theta = 480$, $A_{max} = 5.0$, $\sum^2 = 4 \times 10^{-12}$, $\Omega^2_{max} = -8.9 \times 10^{-5}$, m = 1 unstable.

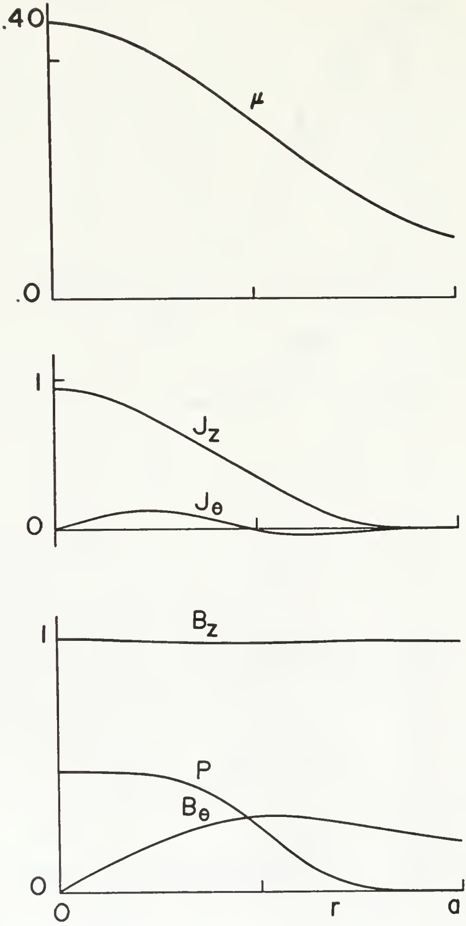

Fig. 7. Tokamak, $\beta = 0.037$, $\beta_\theta = 1.73$, $A_{max} = 2.17$, $\sum{}^2 = 4 \times 10^{-12}$, $\Omega^2_{max} = -1.7 \times 10^{-4}$, m = 1 unstable.

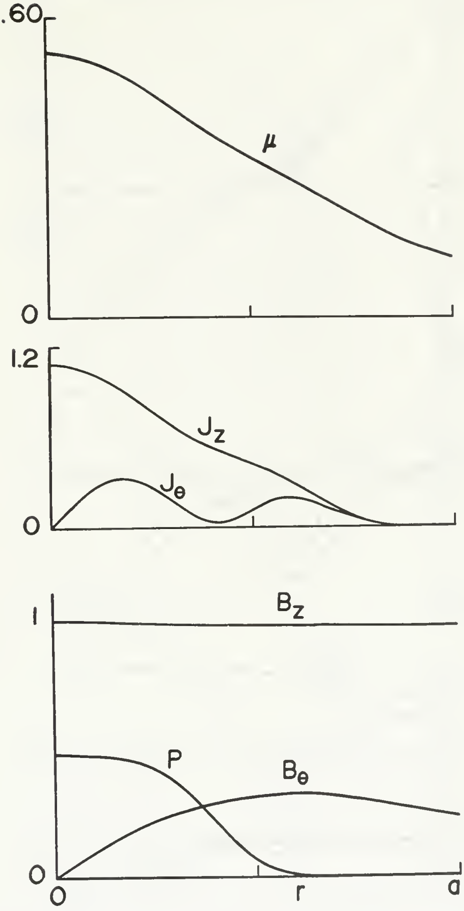

Fig. 8. Tokamak, $\beta = 0.037$, $\beta_\theta = 1.43$, $A_{max} = 1.89$, $\sum^{2} = 4x10^{-12}$, $\Omega^2_{max} = - 5.2 \times 10^{-4}$, no J_θ current reversal, m = 1 unstable.

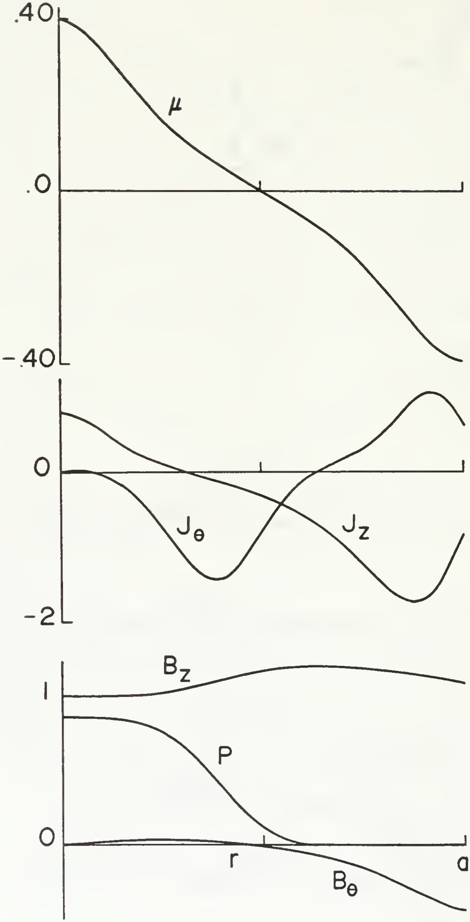

Fig. 9. B_θ-reversed pinch, $\beta = 0.30$, $\beta_\theta = 2.28$, $A_{max} = 2.52$, $\sum^2 = 4 \times 10^{-12}$, $\Omega^2_{max} = -10^{-4}$, m = 1 unstable.

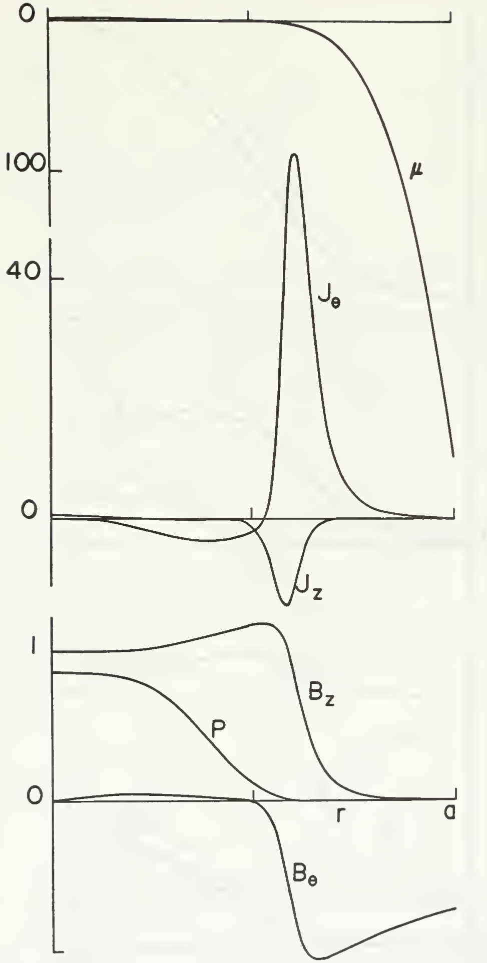

Fig.10. B_θ-reversed pinch, $\beta = 0.30$, $\beta_\theta = 0.38$; $A_{max} = 1.40$, $\sum^2 = 4 \times 10^{-12}$, $\Omega^2_{max} = -9.2 \times 10^{-5}$ and no current at the wall, m = 1 unstable.

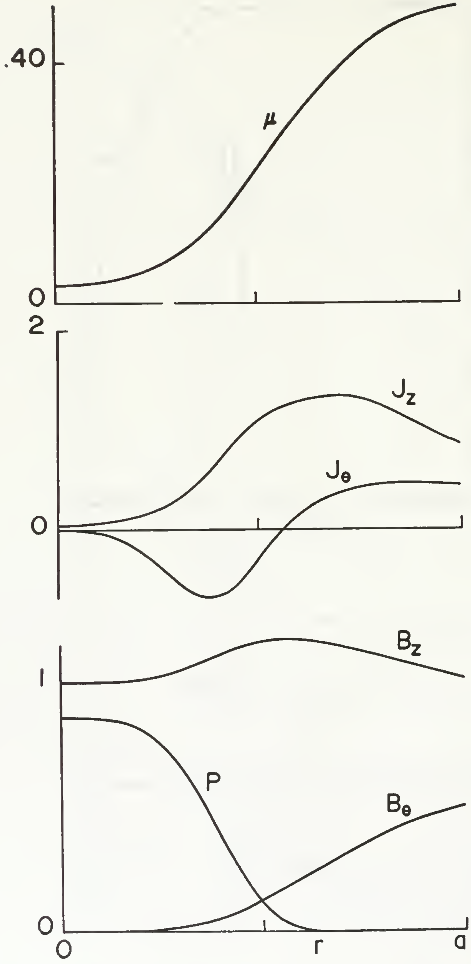

Fig.11. Screw-pinch, $\beta = 0.30$, $\beta_\theta = 1.71$, $A_{max} = 1.89$, $\sum^2 = 4 \times 10^{-12}$, $\Omega^2_{max} = -7.0 \times 10^{-3}$, m = 1 unstable.

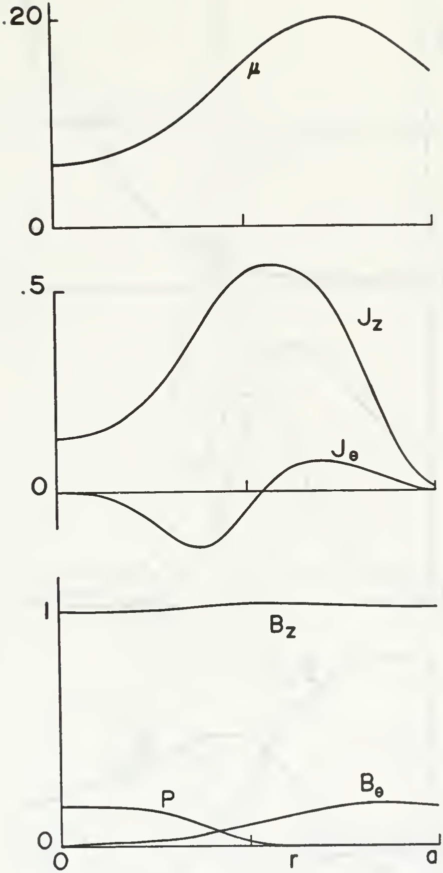

Fig.12. Screw-pinch, $\beta = 0.08$, $\beta_\theta = 2.70$, $A_{max} = 4.50$, $\sum^2 = 3 \times 10^{-7}$, $\Omega^2_{max} = -3.0 \times 10^{-4}$, no current at the wall, $m = 1$ unstable.

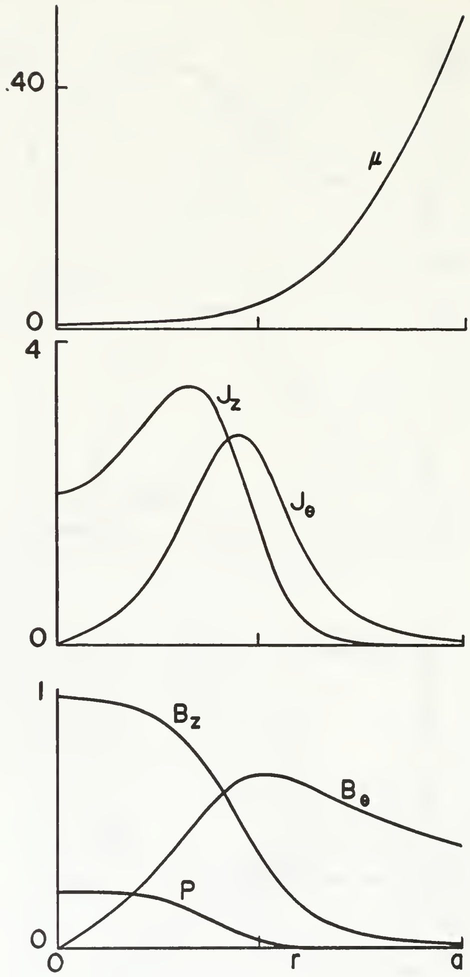

Fig.13. Combined pinch, $\beta = 0.10$, $\beta_\theta = 0.22$, $\sum^2 = 4 \times 10^{-12}$, $m = 1$ stable.

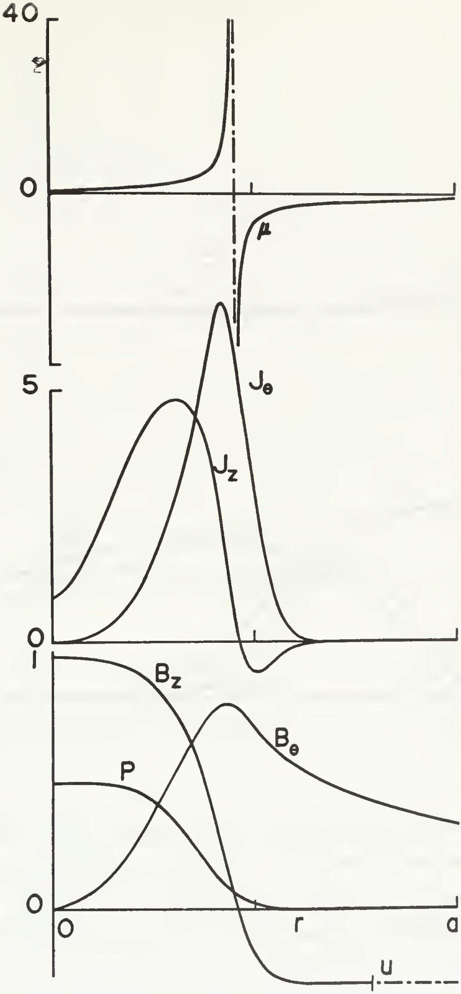

Fig.14. B_z-reversed pinch, $\beta = 0.20$, $\beta_\theta = 0.38$, $\Sigma^2 = 4 \times 10^{-12}$, $m = 1$ stable. It becomes unstable for wall position farther than 0.80a.

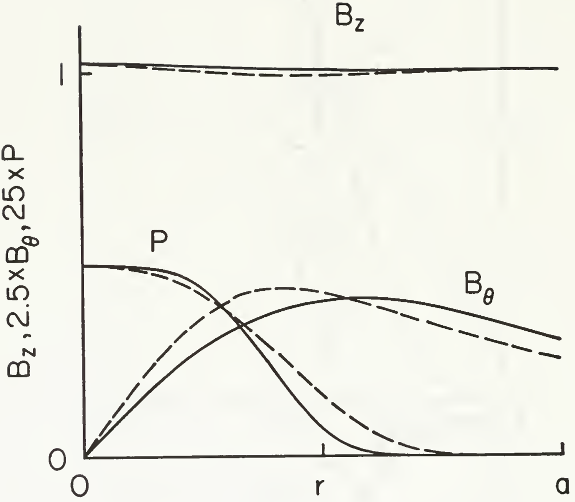

Fig.15. Unstable Tokamak (dotted lines) compared with stable one (solid lines). $\beta = 0.036$, $\beta_\theta = 1.30$, stable one: $\Omega^2_{max} = -5.2 \times 10^{-4}$ (m = 1), $\sum^2 = 10^{-12}$ (m > 1), unstable one: $\Omega^2_{max} = -1.7 \times 10^{-4}$ (m = 1), -6.5×10^{-6} (m = 2), -1.8×10^{-6} (m = 3, -4.7×10^{-7} (m = 4).

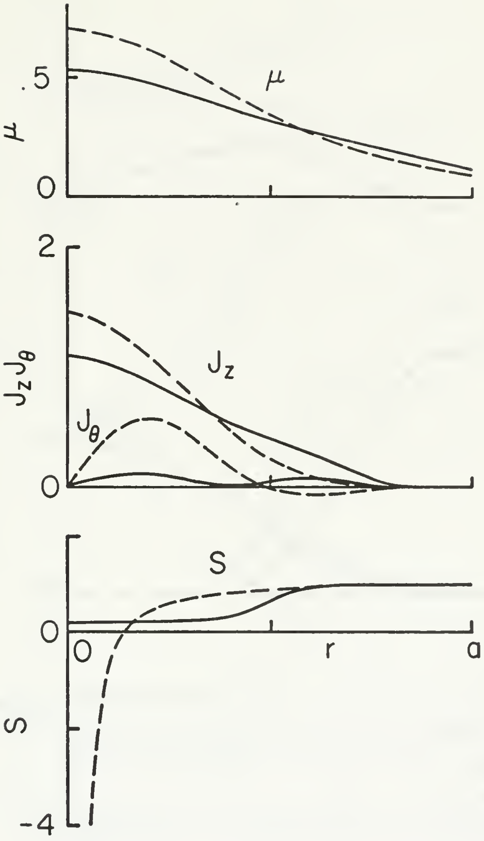

Fig.16. Profiles μ, j_θ, j_z, and Suydam function S for Tokamak configurations of Fig. 15.

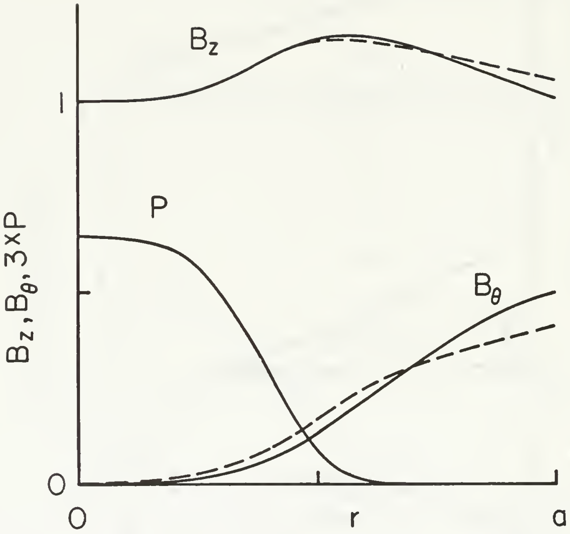

Fig.17. Unstable screw-pinch (dotted lines) compared with stable one (solid lines). $\beta = 0.30$, $\beta_\theta = 2.50$, stable one: $\Omega^2_{max} = -7.0 \times 10^{-3}$ (m = 1), $\Sigma^2 = 4 \times 10^{-12}$ (m > 1), unstable one: $\Omega^2_{max} = -1.2 \times 10^{-2}$ (m = 1), -4.8×10^{-6} (m = 2), -7.8×10^{-6} (m = 3), -8.0×10^{-6} (m = 4).

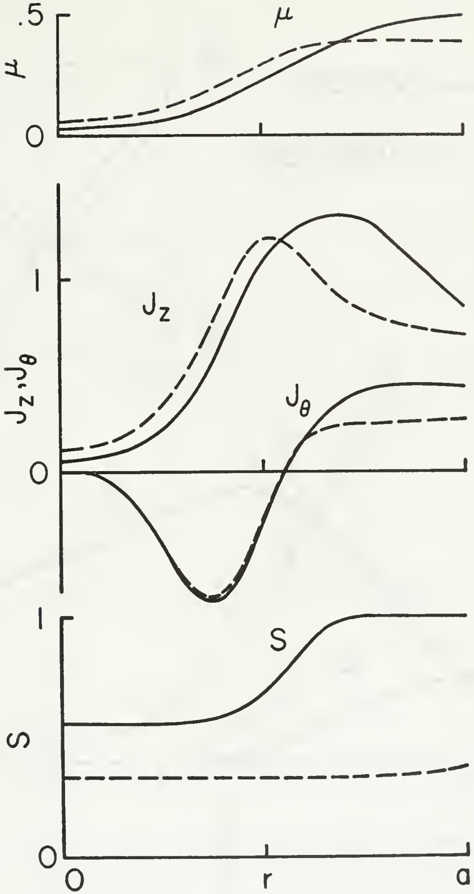

Fig.18. Profiles μ, j_θ, j_z, and S for screw-pinch configurations of Fig. 17.

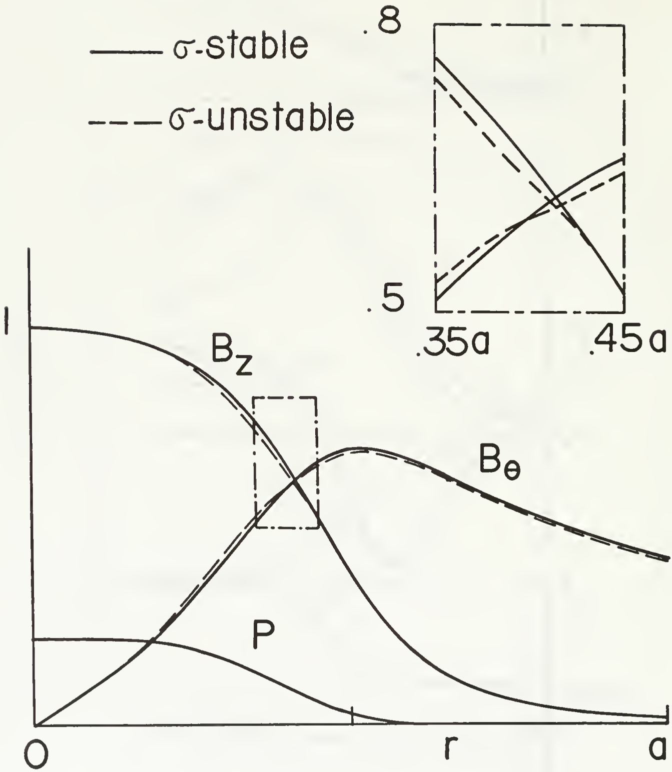

Fig.19. Unstable combined pinch (dotted lines) compared with stable one (solid line). $\beta = 0.10$, $\beta_\theta = 0.23$, stable one: $\sum^2 = 4 \times 10^{-12}$, $m = 1$ stable, unstable one: $\Omega^2_{max} = -3 \times 10^{-4}$ $(m = 1)$.

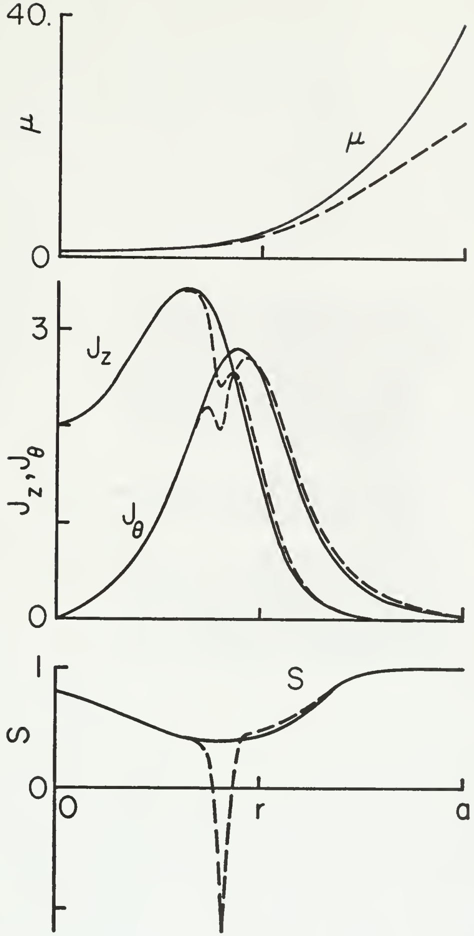

Fig.20. Profiles μ, j_θ, j_z and S for combined pinch configurations of Fig. 19.

This report was prepared as an account of Government sponsored work. Neither the United States, nor the Commission, nor any person acting on behalf of the Commission:

A. Makes any warranty or representation, express or implied, with respect to the accuracy, completeness, or usefulness of the information contained in this report, or that the use of any information, apparatus, method, or process disclosed in this report may not infringe privately owned rights; or

B. Assumes any liabilities with respect to the use of, or for damages resulting from the use of any information, apparatus, method, or process disclosed in this report.

As used in the above, "person acting on behalf of the Commission" includes any employee or contractor of the Commission, or employee of such contractor, to the extent that such employee or contractor of the Commission, or employee of such contractor prepares, disseminates, or provides access to, any information pursuant to his employment or contract with the Commission, or his employment with such contractor.